J. Fluid Mech. (1990), *vol.* 219, *pp.* 545–570
Printed in Great Britain

Laminar flow in twisted pipes

By E. R. TUTTLE
Department of Engineering, University of Denver, Denver CO 80208, USA

(Received 11 August 1989 and in revised form 12 March 1990)

The effect of torsion on fully developed laminar flow in a twisted pipe is considered in the low-Reynolds-number regime. The flow in a pipe of elliptical cross-section whose axis is straight but which is twisted about that axis is examined and the secondary flow pattern found. The helical pipe of circular cross-section is also revisited; in this case, the first-order torsional effect on the streamtubes is verified, and previous conclusions that such an effect would be of higher order are explained.

1. Introduction

While the general subject of flow in curved pipes has been examined by numerous authors, as evidenced by the extensive bibliographies in two recent review articles on the subject by Berger, Talbot & Yao (1983) and Ito (1987), some areas of this subject have received more attention and are better understood than others. One area which has received relatively little attention, and for which the results obtained by various investigators are in apparent conflict, is that of flow in a helically coiled pipe of finite pitch. It is the object of the present investigation to examine this problem in the limit of steady incompressible laminar flow at low Reynolds number in order to resolve the differences between previous results and to begin to understand the phenomena which appear in the secondary flow patterns when a pipe possesses torsion as well as curvature.

We begin by briefly reviewing previous work on the subject. Truesdell & Adler (1970) suggested that, at least for coils with very small pitch, an appropriate approximation could be obtained by replacing the curvature for a toroidal pipe by the curvature for the helical pipe being considered. This was continued by Manlapaz & Churchill (1980) who, although recognizing that the coordinate system they were employing was non-orthogonal, assumed that the effects introduced by the non-orthogonality were negligible in the limit of small pitch. This assumption leads to essentially the same approximation used on an *ad hoc* basis by Truesdell & Adler.

The consequences of non-orthogonality of the natural coordinate system for flow in a helical pipe of circular cross-section were addressed by Wang (1981) and Murata *et al.* (1981). The governing equations generated by these two sets of investigators are the same except for minor differences in nomenclature. On the other hand, because of the non-orthogonality, these equations are necessarily cast in tensor covariant form and the results obtained must be particularly carefully interpreted, as the covariant and contravariant velocity components of the velocity field are not the same. Interestingly enough, Wang concentrates his attention on the contravariant components, while Murata *et al.* concentrate on the covariant components. As a consequence, Wang finds a contribution of $O(\gamma)$, where γ is the dimensionless torsion, in the secondary flow; Murata *et al.*, on the other hand, conclude that the first torsional effect is of $O(\epsilon\gamma)$, where ϵ is the dimensionless curvature. Wang concludes that the two recirculating cells found by Dean (1927, 1928) are subject to a large

distortion at relatively small values of the torsion, and become a single cell for pipes of very moderate pitch. The secondary flow deduced by Murata *et al.* does not consist of distinct recirculating cells at all and must be represented by a distribution of secondary flow velocity vectors.

Germano (1982) avoided the complications connected with non-orthogonal coordinates by the introduction of an orthogonal coordinate system. Carrying out only a first-order expansion (in γ and ϵ), he concluded that there were no first-order torsional effects. Germano's work has been extended by Kao (1987), who, like Murata *et al.*, finds that the secondary flow is again not derivable from a stream function and must be represented by secondary flow velocity vectors. Although Kao claims to address the paradox posed by the conflicting results of Wang and Murata *et al.* and Germano, he actually works only with Germano's equations and does not come to grips with Wang's results.

In the present investigation, we also have chosen to use Germano's coordinate system as a starting point, mainly because it enables us to avoid the interpretation of covariant and contravariant velocity components. This makes it possible to consider the velocity field in terms of ordinary vectors, which are, perhaps, somewhat easier to visualize. The emphasis here is more on physical interpretation of the velocity field than on extended calculation, it being felt that perhaps this would aid in resolving the differences cited above. The aim is to provide a platform from which further calculations at higher values of the Reynolds number (or, alternatively, the curvature and the torsion) can be made. In this context, it has been found most useful to consider pipes of other than circular cross-section. As many pipes are of this type, the issue is of more than academic interest, and the insight thus gained has proved invaluable in understanding the problem and gaining insight into the effect that torsion has on the streamtubes describing the flow.

2. Navier–Stokes and continuity equations along a space curve

Consider a general continuous curve in space described by $\boldsymbol{R}(s)$, where s is the arclength along the curve and $\boldsymbol{I}$, $\boldsymbol{J}$, $\boldsymbol{K}$ are unit vectors in a fixed Cartesian coordinate system:

$$\boldsymbol{R}(s) = X(s)\,\boldsymbol{I} + Y(s)\,\boldsymbol{J} + Z(s)\,\boldsymbol{K}. \tag{1}$$

The Frenet triad of unit vectors, $\boldsymbol{t}$, $\boldsymbol{n}$, $\boldsymbol{b}$, the curvature, κ, and the torsion, τ, are then given by the usual equations:

$$\left.\begin{aligned} \boldsymbol{t} = \frac{\mathrm{d}\boldsymbol{R}}{\mathrm{d}s}, \quad \boldsymbol{n} = \frac{1}{\kappa}\frac{\mathrm{d}\boldsymbol{t}}{\mathrm{d}s}, \quad \boldsymbol{b} = \boldsymbol{t}\times\boldsymbol{n}, \\ \frac{\mathrm{d}\boldsymbol{n}}{\mathrm{d}s} = -\kappa\boldsymbol{t} + \tau\boldsymbol{b}, \quad \frac{\mathrm{d}\boldsymbol{b}}{\mathrm{d}s} = -\tau\boldsymbol{n}. \end{aligned}\right\} \tag{2}$$

In general, $\boldsymbol{t}$, $\boldsymbol{n}$, and $\boldsymbol{b}$ change in direction as one passes along the curve, while $\kappa(s)$ and $\tau(s)$ change in magnitude.

Now consider a pipe with axis described by $\boldsymbol{R}(s)$ whose cross-section in the plane perpendicular to $\boldsymbol{t}$ is invariant as seen by an observer travelling along the curve and rotating with $\boldsymbol{n}$ and $\boldsymbol{b}$. We now wish to find a useful set of Navier–Stokes equations to describe incompressible laminar flow in such a pipe.

Our first consideration must be the choice of a suitable coordinate system. It is clear that s, the arclength along the pipe axis, should be one of the coordinates. The

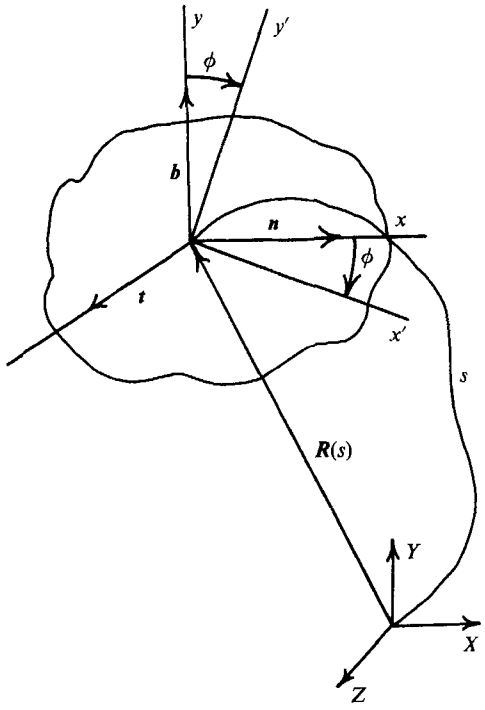

FIGURE 1. Relationships among the coordinate systems employed.

most obvious choice for the other two is the pair x, y such that the position vector can be written in the form

$$\boldsymbol{r} = \boldsymbol{R}(s) + x\boldsymbol{n} + y\boldsymbol{b} = \boldsymbol{R}(s) + x\boldsymbol{i} + y\boldsymbol{j}. \tag{3}$$

This choice is the rectangular analogue of the coordinate system used by Wang (1981). It is, unfortunately, non-orthogonal, as can immediately be seen by forming the infinitesimal

$$\mathrm{d}\boldsymbol{r} = (\mathrm{d}x - \tau y\,\mathrm{d}s)\,\boldsymbol{n} + (\mathrm{d}y + \tau x\,\mathrm{d}s)\,\boldsymbol{b} + (1 - \kappa x)\,\mathrm{d}s\boldsymbol{t}. \tag{4}$$

On the other hand, the boundary of the pipe, expressed in these coordinates, is independent of s, so we can expect the boundary conditions on the pipe flow to be easy to apply. We shall refer to these coordinates as body-centred.

Alternatively, we can select a different pair of coordinates x', y' such that

$$\boldsymbol{r} = \boldsymbol{R}(s) + x'\boldsymbol{i}' + y'\boldsymbol{j}', \tag{5}$$

where $\boldsymbol{i}', \boldsymbol{j}'$ rotate with respect to $\boldsymbol{n}$ and $\boldsymbol{b}$ as one proceeds along the pipe in such a way as just to undo the torsional effect, i.e.

$$\left.\begin{gathered} \frac{\mathrm{d}\boldsymbol{i}'}{\mathrm{d}s} = -\kappa(s)\cos\phi\boldsymbol{t}; \quad \frac{\mathrm{d}\boldsymbol{j}'}{\mathrm{d}s} = -\kappa(s)\sin\phi\boldsymbol{t}; \\ \boldsymbol{i}' \times \boldsymbol{j}' = \boldsymbol{t}; \quad \boldsymbol{i}' \cdot \boldsymbol{j}' = 0; \quad \phi(s) = \int_{s_0}^{s} \tau(s')\,\mathrm{d}s' + \phi_0. \end{gathered}\right\} \tag{6}$$

The relationship between these two coordinate choices is shown in figure 1, for which the tangent vector $\boldsymbol{t}$ is out of the plane of the paper. For convenience, we shall let $\phi_0 = s_0 = 0$. Clearly, in this coordinate system, which we shall refer to as space-

centred, the equation of the pipe boundary is not, in general, independent of s. On the other hand, we can see that, as

$$\mathrm{d}\boldsymbol{r} = \mathrm{d}x'\boldsymbol{i}' + \mathrm{d}y'\boldsymbol{j}' + (1-\kappa x'\cos\phi - \kappa y'\sin\phi)\,\mathrm{d}s\boldsymbol{t}, \tag{7}$$

this coordinate system is orthogonal. This system is the rectangular analogue of that employed by Germano (1982).

Obviously neither system is ideal. One would like to work with an orthogonal system but one would also like to keep invariant boundary conditions and a natural relationship between the cross-sectional equations and the local Frenet triad. The space-centred coordinates x', y', s' have the first property, while the body-centred coordinates x, y, s have the second. (Note that we use s' to denote the arclength coordinate in the space-centred system and s to denote the same coordinate in the body-centred system.) As we shall now see, although no coordinate system possesses all the above features, it is possible, with the aid of physical understanding, to develop a general formulation of the problem which does.

We first consider the x', y', s' system. As this is orthogonal, the equation of continuity and the Navier–Stokes equations can be written in the vector form

$$\boldsymbol{\nabla}' \cdot \boldsymbol{v}' = 0; \quad \frac{\partial \boldsymbol{v}'}{\partial t} + (\boldsymbol{v}' \cdot \boldsymbol{\nabla}')\,\boldsymbol{v}' = -\frac{1}{\rho}\boldsymbol{\nabla}' p - \nu[\boldsymbol{\nabla}' \times (\boldsymbol{\nabla}' \times \boldsymbol{v}')], \tag{8}$$

where ρ is the density, p the pressure, and $\nu = \mu/\rho$ the kinematic viscosity. If we let u', v', w' be the velocity components, then, using standard expressions for the vector operators in a curvilinear orthogonal system (e.g. Batchelor 1967), we obtain our basic equations in the form

$$\frac{\partial}{\partial x'}\left(\frac{u'}{J'}\right) + \frac{\partial}{\partial y'}\left(\frac{v'}{J'}\right) + \frac{\partial w'}{\partial s'} = 0, \tag{9}$$

$$\mathscr{D}'u' + \kappa J' w'^2 \cos\phi = -\frac{1}{\rho}\frac{\partial p}{\partial x'} - \nu\left\{J'\frac{\partial}{\partial y'}\left[\frac{1}{J'}\left(\frac{\partial v'}{\partial x'} - \frac{\partial u'}{\partial y'}\right)\right] - J'\frac{\partial}{\partial s'}\left[J'\frac{\partial u'}{\partial s'} - \frac{\partial w'}{\partial x'} + \kappa J'\cos\phi\, w'\right]\right\}, \tag{10}$$

$$\mathscr{D}'v' + \kappa J' w'^2 \sin\phi = -\frac{1}{\rho}\frac{\partial p}{\partial y'} - \nu\left\{-J'\frac{\partial}{\partial x'}\left[\frac{1}{J'}\left(\frac{\partial v'}{\partial x'} - \frac{\partial u'}{\partial y'}\right)\right] - J'\frac{\partial}{\partial s'}\left[J'\frac{\partial v'}{\partial s'} - \frac{\partial w'}{\partial y'} + \kappa J'\sin\phi\, w'\right]\right\}, \tag{11}$$

$$\mathscr{D}'w' - \kappa J' w'[u'\cos\phi + v'\sin\phi] = -\frac{J'}{\rho}\frac{\partial p'}{\partial s'} - \nu\left\{\frac{\partial}{\partial x'}\left[J'\frac{\partial u'}{\partial s'} - \frac{\partial w'}{\partial x'} + \kappa J'\cos\phi\, w'\right] + \frac{\partial}{\partial y'}\left[J'\frac{\partial v'}{\partial s'} - \frac{\partial w'}{\partial y'} + \kappa J'\sin\phi\, w'\right]\right\}, \tag{12}$$

where

$$\mathscr{D}' \equiv \frac{\partial}{\partial t} + u'\frac{\partial}{\partial x'} + v'\frac{\partial}{\partial y'} + J'w'\frac{\partial}{\partial s'}, \tag{13}$$

and

$$J' \equiv 1/(1-\kappa x'\cos\phi - \kappa y'\sin\phi). \tag{14}$$

The velocity field in the plane perpendicular to the axis of the pipe is given by

$$\tilde{\boldsymbol{v}} = u'\boldsymbol{i}' + v'\boldsymbol{j}', \tag{15}$$

which can also be written as

$$\tilde{\boldsymbol{v}} = \tilde{u}\boldsymbol{n}' + \tilde{v}\boldsymbol{b}', \tag{16}$$

where $\boldsymbol{n}'$ and $\boldsymbol{b}'$ are unit vectors instantaneously coinciding with $\boldsymbol{n}$ and $\boldsymbol{b}$, i.e. coinciding at this particular value of s. It is easy to see that

$$\left.\begin{aligned}\tilde{u} &= u'\cos\phi + v'\sin\phi,\\ \tilde{v} &= -u'\sin\phi + v'\cos\phi.\end{aligned}\right\} \tag{17}$$

Now

$$\left.\begin{aligned}x' &= x\cos\phi - y\sin\phi,\\ y' &= x\sin\phi + y\cos\phi,\\ s' &= s,\end{aligned}\right\} \tag{18}$$

from which we find that

$$\left.\begin{aligned}\frac{\partial}{\partial x'} &= \cos\phi\frac{\partial}{\partial x} - \sin\phi\frac{\partial}{\partial y},\\ \frac{\partial}{\partial y'} &= \sin\phi\frac{\partial}{\partial x} + \cos\phi\frac{\partial}{\partial y},\\ \frac{\partial}{\partial s'} &= \tau y\frac{\partial}{\partial x} - \tau x\frac{\partial}{\partial y} + \frac{\partial}{\partial s}.\end{aligned}\right\} \tag{19}$$

We now rewrite our basic equations (9)–(12) in terms of the velocity components $\tilde{u}, \tilde{v}, \tilde{w}\,(= w')$, all regarded as functions of x, y, s, obtaining

$$\frac{\partial}{\partial x}\left[\frac{\tilde{u}+\tau J y\tilde{w}}{J}\right] + \frac{\partial}{\partial y}\left[\frac{\tilde{v}-\tau J x\tilde{w}}{J}\right] + \frac{\partial w}{\partial s} = 0, \tag{20}$$

$$\begin{aligned}\mathscr{D}\tilde{u} - \tau J\tilde{v}\tilde{w} + \kappa J\tilde{w}^2 = &-\frac{1}{\rho}\frac{\partial p}{\partial x} - \nu\left\{J\frac{\partial}{\partial y}\left[\frac{1}{J}\left(\frac{\partial\tilde{v}}{\partial x} - \frac{\partial\tilde{u}}{\partial y}\right)\right]\right.\\ &\left. - J\frac{\partial}{\partial S}\left[J\frac{\partial\tilde{u}}{\partial S} - \tau J\tilde{v} - \frac{\partial\tilde{w}}{\partial x} + \kappa J\tilde{w}\right] + \tau J\left[J\frac{\partial\tilde{v}}{\partial S} + \tau J\tilde{u} - \frac{\partial\tilde{w}}{\partial y}\right]\right\},\end{aligned} \tag{21}$$

$$\begin{aligned}\mathscr{D}\tilde{v} + \tau J\tilde{u}\tilde{w} = &-\frac{1}{\rho}\frac{\partial p}{\partial y} - \nu\left\{-J\frac{\partial}{\partial x}\left[\frac{1}{J}\left(\frac{\partial\tilde{u}}{\partial x} - \frac{\partial\tilde{u}}{\partial y}\right)\right]\right.\\ &\left. - J\frac{\partial}{\partial S}\left[J\frac{\partial\tilde{v}}{\partial S} + \tau J\tilde{u} - \frac{\partial\tilde{w}}{\partial y}\right] - \tau J\left[J\frac{\partial\tilde{u}}{\partial S} - \tau J\tilde{u} - \frac{\partial\tilde{w}}{\partial x} + \kappa J\tilde{w}\right]\right\},\end{aligned} \tag{22}$$

$$\mathscr{D}\tilde{w} - \kappa J\tilde{u}\tilde{w} = -\frac{J}{\rho}\frac{\partial p}{\partial S} - \nu\left\{\frac{\partial}{\partial x}\left[J\frac{\partial\tilde{u}}{\partial S} - \tau J\tilde{v} - \frac{\partial\tilde{w}}{\partial x} + \kappa J\tilde{w}\right] + \frac{\partial}{\partial y}\left[J\frac{\partial\tilde{v}}{\partial S} + \tau J\tilde{u} - \frac{\partial\tilde{w}}{\partial y}\right]\right\}, \tag{23}$$

where

$$\left.\begin{aligned}\mathscr{D} &\equiv \frac{\partial}{\partial t} + [\tilde{u}+\tau J y\tilde{w}]\frac{\partial}{\partial x} + [\tilde{v}-\tau J x\tilde{w}]\frac{\partial}{\partial y} + J\tilde{w}\frac{\partial}{\partial s},\\ J &\equiv 1/(1-\kappa x),\end{aligned}\right\} \tag{24}$$

and

$$\frac{\partial}{\partial S} \equiv \tau y\frac{\partial}{\partial x} - \tau x\frac{\partial}{\partial y} + \frac{\partial}{\partial s}.$$

It is important to remember that, even though $\tilde{u}, \tilde{v}, \tilde{w}$ expressed as functions of x, y, s are velocity components along axes coinciding instantaneously with $\boldsymbol{n}$, $\boldsymbol{b}$, $\boldsymbol{t}$, this is still a space-centred formulation; $\boldsymbol{n}'$ and $\boldsymbol{b}'$ still rotate with respect to $\boldsymbol{n}$ and $\boldsymbol{b}$. The rates of change of $\boldsymbol{n}$ and $\boldsymbol{b}$ with respect to $\boldsymbol{n}'$ and $\boldsymbol{b}'$ are easily seen to be

$$\frac{\mathrm{d}\boldsymbol{n}}{\mathrm{d}s} = \tau\boldsymbol{b}, \quad \frac{\mathrm{d}\boldsymbol{b}}{\mathrm{d}s} = -\tau\boldsymbol{n}, \tag{25}$$

so the angular velocity of the $\boldsymbol{t}', \boldsymbol{n}', \boldsymbol{b}'$ triad with respect to the $\boldsymbol{t}, \boldsymbol{n}, \boldsymbol{b}$ triad is simply

$$\boldsymbol{\omega} = \tau J \tilde{w} \boldsymbol{t}. \tag{26}$$

From elementary kinematics we now see that

$$\begin{aligned} \tilde{\boldsymbol{v}} &= \tilde{w}\boldsymbol{t}' + \tilde{u}\boldsymbol{n}' + \tilde{v}\boldsymbol{b}', \\ &= w\boldsymbol{t} + (u\boldsymbol{n} + v\boldsymbol{b}) + \tau J w(-y\boldsymbol{n} + x\boldsymbol{b}), \\ &= \boldsymbol{v}_0 + \boldsymbol{v} + \boldsymbol{\omega} \times (x\boldsymbol{i} + y\boldsymbol{j}). \end{aligned} \tag{27}$$

Thus the velocity field $\boldsymbol{v}' = \tilde{\boldsymbol{v}}$ is to be interpreted as the sum of three contributions:

(i) a translational velocity parallel to the axis;

(ii) a velocity in the plane perpendicular to the axis as seen by an observer fixed with respect to the Frenet triad; and

(iii) a rotational velocity caused by the rotation of $\boldsymbol{n}$ and $\boldsymbol{b}$ about the tangent vector $\boldsymbol{t}$. Comparing the two forms of (27), we see that

$$u = \tilde{u} + \tau J y \tilde{w}, \quad v = \tilde{v} - \tau J x \tilde{w}, \quad w = \tilde{w}. \tag{28}$$

Now as u, v, w vanish on the pipe surface, so do $\tilde{u}$, $\tilde{v}$, and $\tilde{w}$, all now expressed as functions of the body-centred coordinates x, y, s.

It can be shown that the velocity field calculated by Germano (1982) is actually the u', v', w' or $\tilde{u}, \tilde{v}, \tilde{w}$ field and that his equations of motion are equivalent to those of (9)–(12). On the other hand, the velocity field calculated by Wang (1981) is the u, v, w field,

$$v^1 = u, \quad v^2 = v, \quad v_3 = wJ,$$

his equations of motion being equivalent to (20)–(23) once $\tilde{u}, \tilde{v}, \tilde{w}$ have been replaced by u, v, w according to the prescription of (28). Note that, to obtain detailed agreement, one must transform (23) to contravariant form.

To conclude this section, let us consider the question of fully developed steady flow and attempt to answer the question of the effect of torsion on the secondary flow found by Dean (1927, 1928). We first set all partials with respect to t equal to zero, as there is no time dependence, and assume that the curvature and torsion are both constant (independent of s). We cannot assume that u', v', w' are independent of s, as the axes $\boldsymbol{i}', \boldsymbol{j}'$ have different orientations with respect to the pipe cross-section at different s. On the other hand, $\tilde{u}, \tilde{v}, \tilde{w}$, and u, v, w are all independent of s, and $p(x, y, s)$ depends on s linearly in lowest order. With these assumptions, the continuity equation (20) reduces to

$$\frac{\partial}{\partial x}\left[\frac{\tilde{u} + \tau J y \tilde{w}}{J}\right] + \frac{\partial}{\partial y}\left[\frac{\tilde{v} - \tau J x \tilde{w}}{J}\right] = 0,$$

or

$$\frac{\partial}{\partial x}\left[\frac{u}{J}\right] + \frac{\partial}{\partial y}\left[\frac{v}{J}\right] = 0. \tag{29}$$

It is easy to see that u and v can be derived from a scalar stream function $\Psi(x, y)$, where

$$u(x, y) = J\frac{\partial \Psi}{\partial y}, \quad v(x, y) = -J\frac{\partial \Psi}{\partial x}. \tag{30}$$

Thus $\Psi(x, y)$ can be used to define secondary flow streamlines of u, v in the (x, y)-plane. We must note that no similar stream function exists for the velocity components $\tilde{u}$, $\tilde{v}$, as the terms in $\tilde{w}$ act as sources and sinks. We also see that a two-

dimensional secondary flow pattern of the Dean type only exists for the observer who moves along the curve and rotates with the normal and binormal, i.e. a body-centred observer. Furthermore, this observer will indeed see the first-order effect on the two recirculating cells which was predicted by Wang (1981). From the point of view of a space-centred observer, $\Psi(x,y) = c_1$ is a surface in three-dimensional space. It is easy to show that

$$(\nabla'\Psi)\cdot \boldsymbol{v}' = 0, \tag{31a}$$

i.e. the normal to the surface $\Psi(x,y) = \Psi(x',y',s') =$ constant is always normal to the velocity $\boldsymbol{v}'$ whose components are u',v',w'. This surface therefore describes a streamtube in the inertial frame X,Y,Z.

On the other hand, the calculation of the flow rate is obviously performed by a body-centred observer, located at a particular plane $s =$ constant, and thus has the form

$$Q = \int_A \tilde{w}\,\mathrm{d}A = \int_{A'} w'\,\mathrm{d}A'. \tag{31b}$$

This is also in agreement with the calculation given by Wang, where it is the covariant axial velocity which is integrated to obtain the total flow rate.

3. Twisted straight pipes

Before considering flow in a helical pipe, for which both κ and τ are non-zero, let us examine steady, fully developed flow in a pipe whose axis is straight, but which is uniformly twisted about that axis, so that the axes fixed in the cross-section advance as one proceeds along the pipe. In this case, in the limit in which the curvature, κ, tends to zero, the twist or torsion, τ, remains finite. This permits us to examine the torsion effects separately from those induced by curvature of the pipe. For τ constant, (20)–(23) are easily reduced and rearranged to the following:

$$\frac{\partial u}{\partial x}+\frac{\partial v}{\partial y} = 0, \tag{32a}$$

$$u\frac{\partial \tilde{u}}{\partial x}+v\frac{\partial \tilde{u}}{\partial y}-\tau w\tilde{v} = -\frac{1}{\rho}\frac{\partial p}{\partial x}+\nu\left\{\frac{\partial^2\tilde{u}}{\partial x^2}+\frac{\partial^2\tilde{u}}{\partial y^2}-\tau^2\tilde{u} + \left(\tau y\frac{\partial}{\partial x}-\tau x\frac{\partial}{\partial y}\right)\left(\tau y\frac{\partial\tilde{u}}{\partial x}-\tau x\frac{\partial\tilde{u}}{\partial y}-2\tau\tilde{v}\right)\right\}, \tag{32b}$$

$$u\frac{\partial \tilde{v}}{\partial x}+v\frac{\partial \tilde{v}}{\partial y}+\tau w\tilde{u} = -\frac{1}{\rho}\frac{\partial p}{\partial y}+\nu\left\{\frac{\partial^2\tilde{v}}{\partial x^2}+\frac{\partial^2\tilde{v}}{\partial y^2}-\tau^2\tilde{v} + \left(\tau y\frac{\partial}{\partial x}-\tau x\frac{\partial}{\partial y}\right)\left(\tau y\frac{\partial\tilde{v}}{\partial x}-\tau x\frac{\partial\tilde{v}}{\partial y}+2\tau\tilde{u}\right)\right\}, \tag{32c}$$

$$u\frac{\partial \tilde{w}}{\partial x}+v\frac{\partial \tilde{w}}{\partial y} = -\frac{1}{\rho}\frac{\partial p}{\partial s}-\frac{\tau y}{\rho}\frac{\partial p}{\partial x}+\frac{\tau x}{\rho}\frac{\partial p}{\partial y}+\nu\left\{\frac{\partial^2\tilde{w}}{\partial x^2}+\frac{\partial^2\tilde{w}}{\partial y^2}+\tau^2\left[y\frac{\partial}{\partial x}-x\frac{\partial}{\partial y}\right]^2\tilde{w}\right\}, \tag{32d}$$

with

$$u = \tilde{u}+\tau y w = \frac{\partial\Psi}{\partial y}, \quad v = \tilde{v}-\tau x w = -\frac{\partial\Psi}{\partial x}. \tag{32e}$$

It is instructive to consider a pipe of elliptical cross-section, for which the untwisted solution is known. Let the pipe be twisted through one complete turn in

the distance $s_T = 2\pi d$, so that $\tau = 1/d$, and let the axes of the ellipse be $2a$ and $2b$, where d is much greater than either a or b. In order to render the governing equations dimensionless, we scale all lengths by a length H, which is of the same order as a and b, all velocities by the centreline velocity U_0, and introduce a Reynolds number based on H, $\mathscr{R} = U_0 H/\nu$; the dimensionless pressure P is then given by $P = pH/(\mu U_0)$, and the dimensionless stream function by $\Phi = \Psi/(U_0 D)$. The length H has been used rather than either a or b in order to emphasize the symmetry in the exchange of X/A with Y/B. We now proceed to solve (32) by the method of successive approximation, using the solution for the straight pipe of elliptical cross-section as the zeroth-order approximation; i.e.

$$W_0 = \left[1-\left(\frac{X}{A}\right)^2-\left(\frac{Y}{B}\right)^2\right], \quad P_0 = -2\left(\frac{1}{A^2}+\frac{1}{B^2}\right)S, \quad U_0 = V_0 = 0. \tag{33}$$

To first order in $\gamma = \tau D$, we find

$$\nabla^4 \Phi_1 = -8\gamma\left(\frac{1}{A^2}+\frac{1}{B^2}\right); \tag{34}$$

and, as Φ_1 must contain the factor $[1-(X/A)^2+(Y/B)^2]^2$ if the no-slip conditions on U and V are to be satisfied, it is easy to show that

$$\left.\begin{aligned} \Phi_1 &= -\frac{\gamma}{\Delta_1}\left(\frac{1}{a^2}+\frac{1}{b^2}\right)\left(1-\frac{X^2}{A^2}-\frac{Y^2}{B^2}\right)^2; \\ \Delta_1 &\equiv \left(\frac{3}{A^4}\right)+\left(\frac{2}{A^2B^2}\right)+\left(\frac{3}{B^4}\right). \end{aligned}\right\} \tag{35}$$

Substitution of U_1 and V_1 into the axial flow equation then yields the result $W_1 = 0$. This is a consequence of the symmetry of this particular cross-section, and will not be true in general. It is clear that U_1 and V_1 do not vanish as $B \to A$; as the body-centred observer rotates counterclockwise, he must see the fluid rotating clockwise. On the other hand, the instantaneous velocity projections and the pressure as given by

$$\left.\begin{aligned} \tilde{U}_1 &= -\Gamma\left(\frac{3}{A^2}+\frac{1}{B^2}\right)Y\left(1-\frac{X^2}{A^2}-\frac{Y^2}{B^2}\right), \\ \tilde{V}_1 &= -\Gamma\left(\frac{1}{A^2}+\frac{3}{B^2}\right)X\left(1-\frac{X^2}{A^2}-\frac{Y^2}{B^2}\right), \\ P_1 &= -2\Gamma XY\left[\frac{3}{A^4}+\frac{10}{A^2B^2}+\frac{3}{B^4}\right], \end{aligned}\right\} \tag{36}$$

where

$$\Gamma \equiv \frac{\gamma}{\Delta_1}\left(\frac{1}{A^2}-\frac{1}{B^2}\right), \tag{37}$$

vanish in this limit and so, therefore, do the space-centred velocities U' and V'. We should also note that, if $A = B$, then

$$\left.\begin{aligned} W_0 &= \left[1-\left(\frac{X^2+Y^2}{A^2}\right)\right], \quad P_0 = -4S, \\ \Phi_1 &= -\frac{\gamma}{A^2}\left[1-\frac{(X^2+Y^2)}{A^2}\right]^2, \end{aligned}\right\} \tag{38}$$

is an exact solution of (32), as indeed it should be.

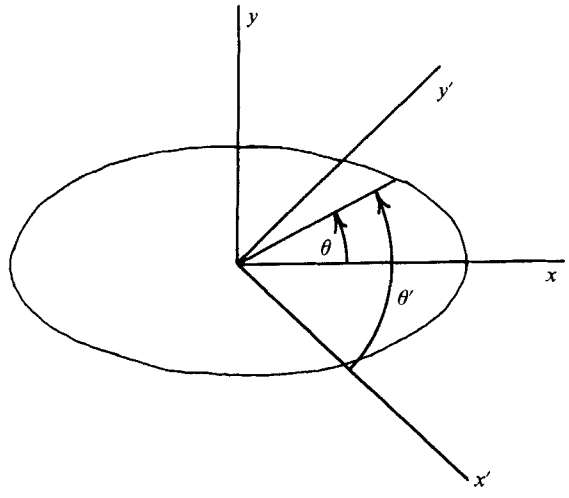

FIGURE 2. Angle of advance of fluid from the points of view of the body-centred observer (θ) and the space-centred observer (θ').

For this very simple problem, in this order, it is possible to find the analytic equations for the streamlines. On the streamline for which

$$\frac{X^2}{A^2}+\frac{Y^2}{B^2}=C^2, \tag{39}$$

we find that $$X = CA\cos(\gamma\alpha S+\phi_0), \quad Y=-CB\sin(\gamma\alpha S+\phi_0), \tag{40}$$

where $$\alpha \equiv \frac{4}{AB\Delta_1}\left(\frac{1}{A^2}+\frac{1}{B^2}\right), \tag{41}$$

which become, in the space-centred system,

$$\left.\begin{aligned} X' &= \tfrac{1}{2}ABC[-A_-\cos(\omega_+ S+\phi_0)+A_+\cos(\omega_- S-\phi_0)],\\ Y' &= \tfrac{1}{2}ABC[-A_-\sin(\omega_+ S+\phi_0)+A_+\sin(\omega_- S-\phi_0)], \end{aligned}\right\} \tag{42}$$

where $$A_\pm = \left(\frac{1}{A}\pm\frac{1}{B}\right), \quad \omega_\pm = A_\pm^2\,\Omega_0 = \gamma(1\pm\alpha), \quad \Omega_0 = \frac{\gamma}{\Delta_1}\left(\frac{3}{A^2}-\frac{2}{AB}+\frac{3}{B^2}\right). \tag{43}$$

As, in general, the ratio ω_+/ω_- is not rational, a two-dimensional plot of X' *vs.* Y' is neither periodic nor closed.

By looking at such a streamline in polar coordinates we can see how rapidly it wraps itself around the axis of the pipe (cf. figure 2). From the body-centred point of view this involves an examination of the angle θ, given by

$$\theta = \tan^{-1}\left(\frac{Y}{X}\right) = -\tan\left(\frac{B}{A}\tan(\gamma\alpha S)\right). \tag{44}$$

For a pipe with a right-handed twist ($\gamma > 0$) it is easy to see that

$$\omega \equiv \frac{\mathrm{d}\theta}{\mathrm{d}S} = -BA\gamma\alpha\frac{C^2}{(X^2+Y^2)} \tag{45}$$

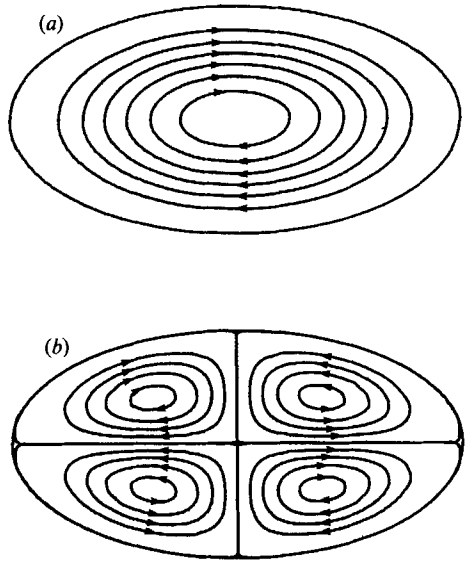

FIGURE 3. Contours of the secondary flow in an elliptical pipe. (*a*) Contours of the first-order solution Φ_1. (*b*) Contours of the second-order solution, Φ_2.

is always negative and the streamline always appears to progress clockwise. From the space-centred system, however,

$$\theta' = \tan^{-1}(Y'/X') = \gamma S + \theta, \tag{46}$$

and

$$\omega' = \frac{\mathrm{d}\theta'}{\mathrm{d}S} = \gamma\left\{1 - 4\left(\frac{1}{A^2}+\frac{1}{B^2}\right)\frac{C^2}{\Delta_1(X^2+Y^2)}\right\}, \tag{47}$$

which may be either positive or negative. As a matter of fact, although θ' does increase with S in the long run, there are always local regions of retrograde motion.

None of the results obtained thus far for the secondary flow involve the inertial terms. By continuing the calculations to second order in γ we obtain the first inertial contributions and, thus, the first distortions of the twisted elliptical streamtubes and the first direct dependence on $\mathscr{R}$. Without going into detail, we find that

$$\Phi_2 = \Lambda\left[1-\left(\frac{X}{A}\right)^2-\left(\frac{Y}{B}\right)^2\right]^2\frac{X}{A}\frac{Y}{B}\left[C_0+C_x\left(\frac{X}{A}\right)^2+C_y\left(\frac{Y^2}{B}\right)\right], \tag{48}$$

where

$$\left.\begin{aligned}
\Lambda &\equiv \frac{4\gamma^2\mathscr{R}}{120\Delta_1^2}\left(\frac{1}{A^2}-\frac{1}{B^2}\right)AB\left[\frac{9}{A^8}+\frac{28}{A^6B^2}+\frac{54}{A^4B^4}+\frac{28}{A^2B^6}+\frac{9}{B^8}\right]\\
&\quad\times\left[\frac{7}{A^8}+\frac{28}{A^6B^2}+\frac{58}{A^4B^4}+\frac{28}{A^2B^6}+\frac{7}{B^8}\right]^{-1},\\
C_0 &\equiv -\left[\frac{25}{A^8}+\frac{84}{A^6B^2}+\frac{166}{A^4B^4}+\frac{84}{A^2B^6}+\frac{25}{B^8}\right]\left[\frac{5}{A^4}+\frac{6}{A^2B^2}+\frac{5}{B^4}\right]^{-1},\\
C_x &\equiv \left[\frac{1}{A^4}+\frac{2}{A^2B^2}+\frac{5}{B^4}\right],\quad C_y \equiv \left[\frac{5}{A^4}+\frac{2}{A^2B^4}+\frac{1}{B^4}\right].
\end{aligned}\right\} \tag{49}$$

Figure 3(*a*, *b*) shows separate plots of Φ_1 and Φ_2, the arrows indicating the direction of flow from the point of view of the observer who moves along the axis of

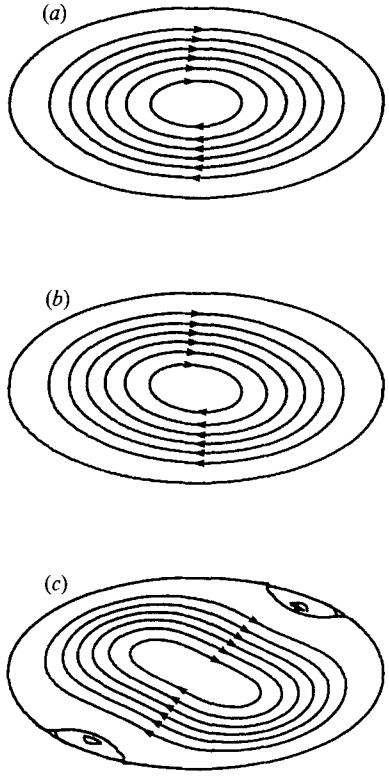

FIGURE 4. Superposition of the secondary flow contours for (*a*) $\gamma\mathscr{R} = 0.1$, (*b*) $\gamma\mathscr{R} = 5$, and (*c*) $\gamma\mathscr{R} = 40$.

the pipe and rotates with it so that the cross-section is always oriented as shown. (In all the plots in the remainder of this section the ratio of semi-minor to semi-major axes, B/A, is taken to be 0.5.) In each case the contours are equally spaced. The plot of Φ_1 shows the familiar and expected elliptical contours, though it should be noted that the spacing is quadratic, rather than linear. The plot of Φ_2 yields four circulating cells; those in the first and third quadrants have positive values of Φ_2 and counterclockwise flow, while those in the second and fourth quadrants have negative values and clockwise flow.

Figure 4 shows the effect of superposition of the two contributions for three values of the parameter $\gamma\mathscr{R}$ using $H = A$, namely $\gamma\mathscr{R} = 0.1$, 5 and 40. (As in the Dean case for flow in a toroidal pipe, higher-order terms in this problem tend to be associated with characteristic denominators; for the torsion terms this number seems to be 120.) For $\gamma\mathscr{R} = 0.1$, the pattern is indistinguishable from that for Φ_1, as seen in figure 4(*a*). For $\gamma\mathscr{R} = 5$, the pattern is distorted, but clearly displays its elliptical origin. In figure 4(*c*), the distortion is sufficient to cause the appearance of small counterclockwise rotating cells. These last should not be taken very seriously, as $\gamma\mathscr{R} = 40$ is probably beyond the range of validity of the current approximation; higher-order terms will have almost certainly become important by this time. Although the main flow contours have approximately equal spacing, the counterflow contour shown has only $\frac{1}{10}$ the main-flow spacing.

One can also find the second-order component of the axial flow W_2; this consists of a non-inertial part containing terms of up to fourth order in X and Y and an inertial contribution containing terms of up to tenth order in the same quantities. It is

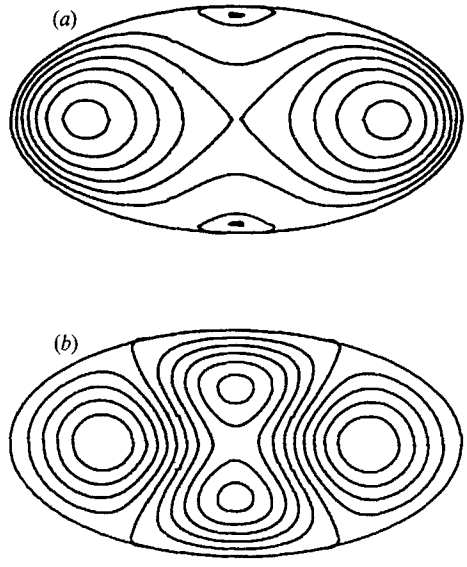

FIGURE 5. Contours of the distortion of the axial flow. (*a*) Non-inertial contribution. (*b*) Inertial contribution.

relatively easy to find the three non-inertial coefficients in the expression for the non-inertial contribution to W_2. On the other hand, the 15 equations for the 15 coefficients appearing in the inertial contribution are sufficiently complicated that it has been found more convenient to find these numerically for each assumed value of the ratio B/A. The details of this calculation are given in Appendix A. Figure 5 gives plots of the non-inertial (figure 5*a*) and inertial (figure 5*b*) contributions to W_2. The non-inertial part of W_2 is negative everywhere except in the two small areas at the ends of the minor axis of the ellipse, while the inertial part is negative in the central portion and positive in the two regions on opposite ends of the major axis. As both contributions are proportional to γ^2, their relative size depends only on the Reynolds number. Figure 6 shows the development of the total W_2 contribution for $\mathscr{R} = 0.1$, 10, and 40; the contributions are negative in most of the flow field. To obtain the full axial velocity pattern, one must add to this the unperturbed flow field $W_0 = (1-X^2/A^2-Y^2/B^2)$. When this has been done, one finds that the entire field is positive, at least for any reasonable (small) values of γ; and, as these are all second-order contributions, the apparent distortion of the axial flow is too small to observe on a contour plot of this type.

Finally, one can find the change in the flow rate by integrating W_2 over the elliptical cross-section. One finds that the inertial part of W_2 yields no change in total flow rate (one can show that the first inertial contribution will not appear until fourth order in γ), but that the non-inertial part yields a decrease in flow rate given by

$$\frac{\Delta Q}{Q_s} = -\frac{4A^2B^2\gamma^2}{\Delta_1}\left(\frac{1}{A^2}-\frac{1}{B^2}\right)^2\left(\frac{1}{A^2}+\frac{1}{B^2}\right), \tag{50}$$

which clearly vanishes in the limit of a circular pipe.

The problem of the elliptical pipe has also been studied by Todd (1977). He uses governing equations which can be reduced to (20)–(23) above, and solves for the space-centred transverse velocity field $\tilde{U}, \tilde{V}$ to first order, and for the longitudinal velocity field to second order. While he realizes that the velocity across the main flow

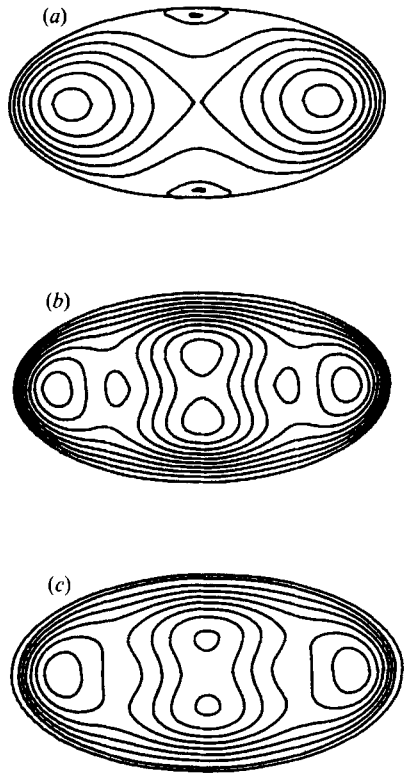

FIGURE 6. Contours of the total second-order contributions to the axial flow. (*a*) $\mathscr{R} = 0.1$, (*b*) $\mathscr{R} = 10$, (*c*) $\mathscr{R} = 40$.

must be modified, he does not appear to recognize that the 'correction factor' is, in reality, general and involves more than the longitudinal flow in the untwisted pipe. The longitudinal velocity profiles appear to agree with those given here.

4. Helical pipe flow

Finally, we address the question of fully developed flow in a helical pipe of circular cross-section, which is the problem considered by Wang (1981), Germano (1982), and Kao (1987). It is convenient to change to polar rather than rectangular coordinates, as shown in figure 7, and to make all equations dimensionless by referring all lengths to a, the pipe radius, all velocities to U_0, the centreline axial velocity in pure Poiseuille flow, and the pressure to $\mu U_0/a$. Thus

$$\left.\begin{gathered} \eta \equiv \frac{r}{a}, \quad x \equiv \frac{s}{a}, \quad \epsilon \equiv \kappa a, \quad \gamma \equiv \tau a, \\ u \equiv U_0 U, \quad v \equiv U_0 V, \quad w \equiv U_0 W, \quad p \equiv \frac{\mu U_0}{a} \Pi, \quad \mathscr{R} \equiv U_0 a/\nu, \\ \text{and} \qquad \theta' = \theta + \phi + \tfrac{1}{2}\pi, \quad \frac{\partial}{\partial s'} = \frac{\partial}{\partial s} + \tau \frac{\partial}{\partial \theta}. \end{gathered}\right\} \tag{51}$$

The velocities analogous to those of §2 can then be shown to be

$$U' = \tilde{U} = U, \quad V' = \tilde{V} = V + \gamma\eta W/(1 + \epsilon\eta \sin\theta), \quad W' = \tilde{W} = W, \tag{52}$$

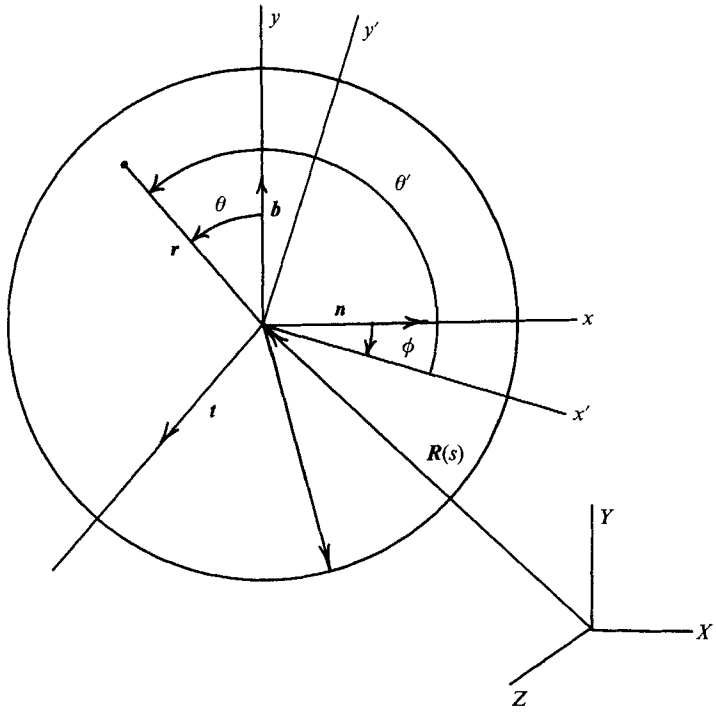

FIGURE 7. Coordinates used for analysis of flow in a helical pipe of circular cross-section.

and the basic equations for steady, fully developed flow equivalent to (20)–(23) become

$$\frac{1}{\eta}\frac{\partial}{\partial\eta}\left[\frac{\eta\tilde{U}}{J}\right]+\frac{1}{\eta}\frac{\partial}{\partial\theta}\left[\frac{\tilde{V}-\gamma\eta J\tilde{W}}{J}\right]=0, \tag{53a}$$

$$\mathscr{D}\tilde{U}-\frac{\tilde{V}^2}{\eta}-\epsilon J\sin\theta\tilde{W}^2=-\frac{\partial\Pi}{\partial\eta}-\frac{1}{\mathscr{R}}\left\{\frac{J}{\eta}\frac{\partial}{\partial\theta}\left[\frac{1}{J}\left(\frac{\partial\tilde{V}}{\partial\eta}+\frac{\tilde{V}}{\eta}-\frac{1}{\eta}\frac{\partial\tilde{U}}{\partial\theta}\right)\right]\right.$$
$$\left.+\gamma J\frac{\partial}{\partial\theta}\left[-J\gamma\frac{\partial\tilde{U}}{\partial\theta}-\frac{\partial\tilde{W}}{\partial\eta}-\epsilon J\sin\theta\tilde{W}\right]\right\}, \tag{53b}$$

$$\mathscr{D}\tilde{V}+\frac{\tilde{U}\tilde{V}}{\eta}-\epsilon J\cos\theta\tilde{W}^2=-\frac{1}{\eta}\frac{\partial\Pi}{\partial\theta}-\frac{1}{\mathscr{R}}\left\{-J\frac{\partial}{\partial\eta}\left[\frac{1}{J}\left(\frac{\partial\tilde{V}}{\partial\eta}+\frac{\tilde{V}}{\eta}-\frac{1}{\eta}\frac{\partial\tilde{U}}{\partial\theta}\right)\right]\right.$$
$$\left.-\gamma J\frac{\partial}{\partial\theta}\left[\gamma J\frac{\partial\tilde{V}}{\partial\theta}+\frac{1}{\eta}\frac{\partial\tilde{W}}{\partial\eta}+\epsilon J\cos\theta\tilde{W}\right]\right\}, \tag{53c}$$

$$\mathscr{D}\tilde{W}+\epsilon J(\sin\theta\tilde{U}+\cos\theta\tilde{V})\tilde{W}=-J\frac{\partial\Pi}{\partial x}+\gamma J\frac{\partial\Pi}{\partial\theta}$$
$$-\frac{1}{\mathscr{R}}\left\{\left(\frac{\partial}{\partial\eta}+\frac{1}{\eta}\right)\left[-\gamma J\frac{\partial\tilde{U}}{\partial\theta}-\frac{\partial\tilde{W}}{\partial\eta}-\epsilon J\sin\theta\tilde{W}\right]\right.$$
$$\left.+\frac{1}{\eta}\frac{\partial}{\partial\theta}\left[-\gamma J\frac{\partial\tilde{V}}{\partial\theta}-\frac{1}{\eta}\frac{\partial\tilde{W}}{\partial\theta}-\epsilon J\cos\theta\tilde{W}\right]\right\}, \tag{53d}$$

where

$$\left.\begin{aligned}\mathscr{D}&\equiv\tilde{U}\frac{\partial}{\partial\eta}+[\tilde{V}-\gamma J\eta\tilde{W}]\frac{1}{\eta}\frac{\partial}{\partial\theta},\\ J&\equiv 1/(1+\epsilon\eta\sin\theta).\end{aligned}\right\} \tag{53e}$$

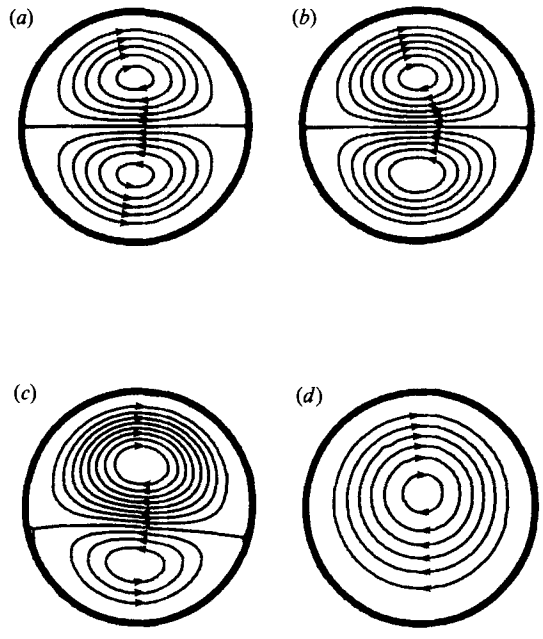

FIGURE 8. Contour plots of the stream function Φ for (*a*) $\epsilon = 0.1$, $\gamma = 0$; (*b*) $\epsilon = 0.099$, $\gamma = 0.0099$; (*c*) $\epsilon = 0.05$, $\gamma = 0.05$; (*d*) $\epsilon = 0.0099$, $\gamma = 0.099$; all for $\mathscr{R} = 100$. All contours are equally spaced.

Except for minor changes in nomenclature, these are the same as the basic equations formulated by Germano (1982), with $\tilde{U}$, $\tilde{V}$, $\tilde{W}$ being his velocity components. If one now makes a change of dependent variables from $\tilde{U}$, $\tilde{V}$, $\tilde{W}$ to U, V, W and performs some rather tedious manipulations, one can obtain the equations of motion given by Wang (1981), with

$$U = u = v^1, \quad V = v = \eta v^2, \quad WJ = v_3.$$

In other words, Germano and Wang are simply considering the same velocity field, but from different points of view.

We must now select a suitable perturbation scheme. Both Wang and Germano use an expansion in powers of the parameter $\epsilon = \kappa a$, including the torsional effects through the ratio $\tau/\kappa = \lambda$; Kao (1987) includes these in the expansion parameter $\beta = a\tau^2/(2\kappa)$. In all cases, these ratios are assumed to be at most of $O(1)$. However, as we saw in the previous section, for a problem in which both parameters given above tend to infinity, it is quite possible to consider situations in which the curvature tends to zero while the torsion remains finite. We have found it both useful and instructive to be able to keep this as a possible limit. We therefore consider an expansion in the two parameters ϵ and γ and take each of the dependent variables to be given by a series of the form

$$\begin{aligned} F = {} & F_{00} + \epsilon F_{01} + \epsilon^2 F_{02} + \ldots \\ & + \gamma F_{10} + \epsilon\gamma F_{11} + \gamma\epsilon^2 F_{12} + \ldots \\ & + \ldots, \end{aligned} \tag{54}$$

in which the first subscript indicates the associated power of γ and the second, the

associated power of ϵ, both considered to be much less than 1. Returning to Wang's and Germano's results, we see that their calculations actually include the terms

$$F \approx F_{00} + \epsilon F_{01} + \gamma F_{10}, \tag{55}$$

where F_{00} represents the Poiseuille flow in a straight pipe and ϵF_{01}, the first-order Dean flow. Germano finds that, from his point of view, all $\gamma F_{10} = 0$, while Wang finds

$$U_{10} = W_{10} = \Pi_{10} = 0, \quad V_{10} = \eta(\eta^2 - 1) = -\eta W_{00}, \tag{56}$$

in agreement with the prescription of (52). The two results are thus completely consistent with each other.

It is instructive to find the $\epsilon\gamma F_{11}$ terms; these represent the lowest-order distortion of the Dean flow by the torsion. In the approximation

$$F \approx F_{00} + \epsilon F_{01} + \gamma F_{10} + \epsilon\gamma F_{11}, \tag{57}$$

we obtain the following:

$$\Phi = \epsilon \frac{\mathscr{R}}{288}(\eta^7 - 6\eta^5 + 9\eta^3 - 4\eta)\cos\theta - \tfrac{1}{4}\gamma(\eta^4 - 2\eta^2 + 1) + \tfrac{1}{6}\epsilon\gamma(\eta^5 - 2\eta^3 + \eta)\sin\theta$$

$$- \frac{\epsilon\gamma\mathscr{R}^2}{(288)(240)}(\eta^{11} - 9\eta^9 + 30\eta^7 - 50\eta^5 + 41\eta^3 - 13\eta)\sin\theta, \tag{58}$$

$$W = (1 - \eta^2) + \tfrac{3}{4}\epsilon(\eta^3 - \eta)\sin\theta$$

$$+ \frac{e\mathscr{R}^2}{(288)(40)}(\eta^9 - 10\eta^7 + 30\eta^5 - 40\eta^3 + 19\eta)\sin\theta$$

$$+ \frac{\epsilon\gamma\mathscr{R}}{576}(3\eta^7 - 8\eta^5 - 24\eta^3 + 29\eta)\cos\theta$$

$$+ \frac{\epsilon\gamma\mathscr{R}^3}{(288)^2(350)}(20\eta^{13} - 294\eta^{11} + 1575\eta^9 - 4550\eta^7$$

$$+ 7630\eta^5 - 7350\eta^3 + 2969\eta)\cos\theta, \tag{59}$$

$$\Pi = -4x + \tfrac{1}{12}\epsilon(2\eta^5 - 6\eta^3 + 9\eta)\sin\theta + \frac{\epsilon\gamma}{6\mathscr{R}}(3\eta^3 - \eta)\cos\theta$$

$$+ \frac{\epsilon\gamma\mathscr{R}}{(240)(72)}(3\eta^9 - 30\eta^7 + 90\eta^5 - 120\eta^3 + 101\eta)\cos\theta. \tag{60}$$

The transverse body-centred velocities U and V are obtained from the function Φ as follows:

$$U = J\frac{1}{\eta}\frac{\partial\Phi}{\partial\theta}, \quad V = -J\frac{\partial\Phi}{\partial\eta}, \tag{61}$$

and the transverse space-centred velocities $\tilde{U}$ and $\tilde{V}$ can be obtained from these through (52).

Figures 8, 9, and 10 illustrate the results obtained above. At the low values of Reynolds number required for these to be significant, it is easy to see that the second-order term in Φ which is dependent only on γ rapidly dominates the transverse flow pattern, as predicted by Wang (1981), while the equivalent terms in W and Π show a much weaker effect. The plots of W, if rotated so that the dividing lines coincide, are almost indistinguishable from each other; the same is true of the plots of Π. Thus

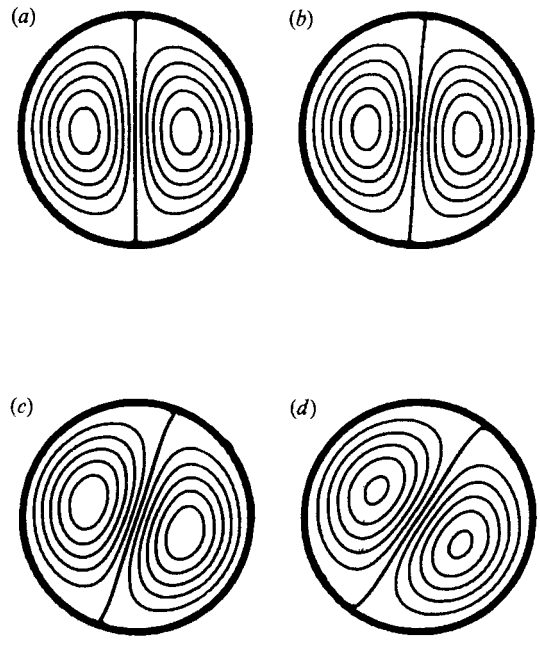

FIGURE 9. Contour plots of the change in axial flow ΔW for (*a*) $\epsilon = 0.1$, $\gamma = 0$; (*b*) $\epsilon = 0.099$, $\gamma = 0.0099$; (*c*) $\epsilon = 0.05$, $\gamma = 0.05$; (*d*) $\epsilon = 0.0099$, $\gamma = 0.099$; all for $\mathscr{R} = 100$. All contours are equally spaced.

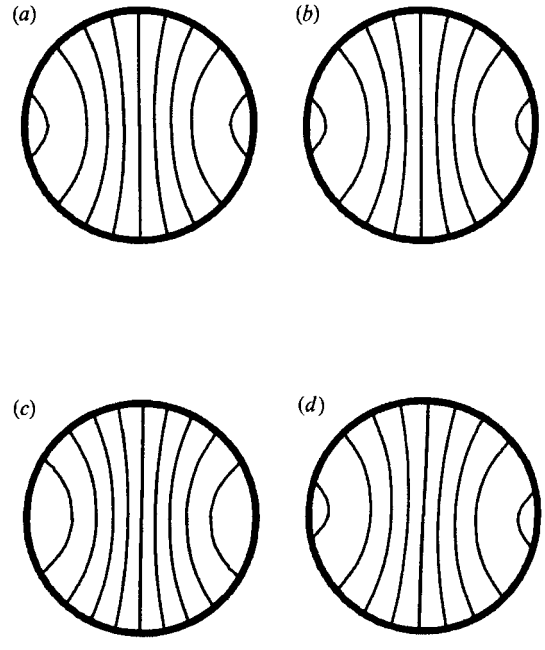

FIGURE 10. Contour plots of the pressure change $\Delta\Pi$ for (*a*) $\epsilon = 0.1$, $\gamma = 0$; (*b*) $\epsilon = 0.099$, $\gamma = 0.0099$; (*c*) $\epsilon = 0.05$, $\gamma = 0.05$; (*d*) $\epsilon = 0.0099$, $\gamma = 0.099$; all for $\mathscr{R} = 100$. All contours are equally spaced.

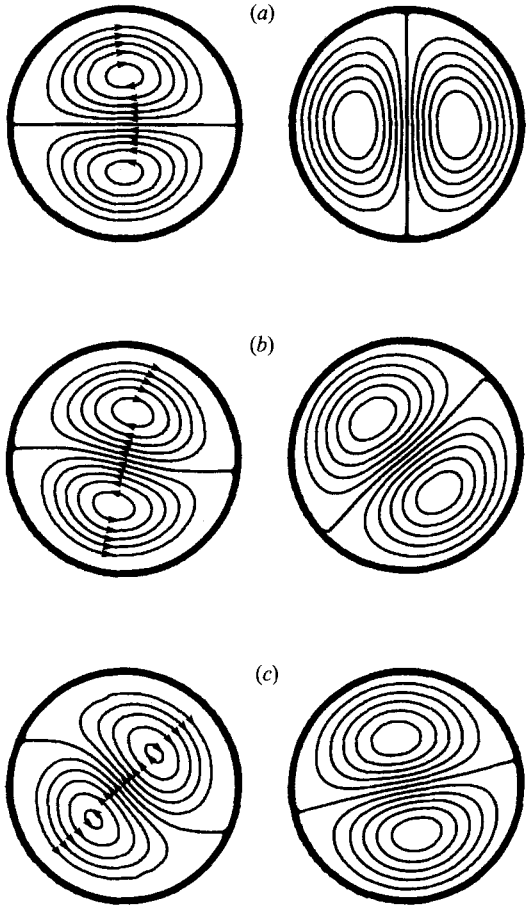

FIGURE 11. Simulation of the effects of torsion on the Dean circulating cells: contours of Φ_D (left) and ΔW_D (right). (a) $\gamma\mathscr{R}/240 = 0$, (b) $\gamma\mathscr{R}/240 = \frac{1}{12}$, (c) $\gamma\mathscr{R}/240 = \frac{1}{3}$.

at very low Reynolds numbers, the torsion very rapidly becomes the dominant factor in the transverse flow pattern and can, for moderate values of the torsion, cause the coalescence of the two recirculating Dean cells.

In order to analyse the torsional effect at higher Reynolds numbers, where the second term in Φ is less dominant, one should either extend the perturbation solution to considerably higher orders in ϵ and γ, following the example of Larrain & Bonilla (1970), or, alternatively, attempt a numerical solution of the full set of governing equations (53). While such calculations are clearly possible, they are also beyond the scope of the present analysis. In addition, the effect of torsion in that case becomes confused with the effect of higher-order terms in the Dean solution for a toroidal pipe, thus obscuring the phenomenon being examined. We have therefore considered instead the effect produced in the limit in which those terms in $(\epsilon^n\gamma^m\mathscr{R}^{n+m})$ dominate the velocity field in the approximation obtained so far. In (58) for the stream function Φ, these are the first and last terms; in (59) for W, the third and last (we again consider only the perturbation to the Poiseuille flow); and in (60) for Π, the second and last terms. By varying the quantity $\gamma\mathscr{R}/240$, we can now see the distortion of the first-order Dean flow by torsion. The results are shown in figures 11 and 12; figure 11 shows the contours of Φ and W, while figure 12 shows those for Π.

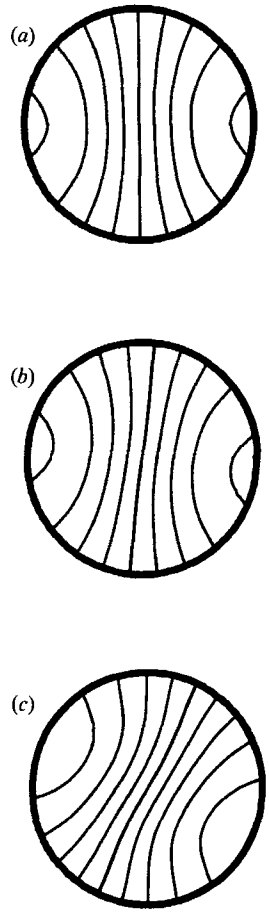

FIGURE 12. Simulation of the effects of torsion on the Dean circulating cells: contours of $\Delta\Pi$. (*a*) $\gamma\mathscr{R}/240 = 0$, (*b*) $\gamma\mathscr{R}/240 = \frac{1}{12}$, (*c*) $\gamma\mathscr{R}/240 = \frac{1}{3}$.

It is clear that the main effect is one of rotation of the flow pattern, the distortion being clearly secondary.

Finally, we would like to find the effect of torsion on the flow rate. It is obvious from the form of $\tilde{W}_{11}$ that there is no change of $O(\epsilon\gamma)$, in agreement with the conclusion reached by Wang (1981). Before we embark on a great deal of tedious algebra, it is useful to analyse the original governing equations (53) to determine exactly what calculations are likely to be necessary. We can make use of the same type of technique used by Larrain & Bonilla (1970) to determine the angular dependence of all the terms in the series solution (54). Table 1 gives these for all $F_{i,j}$ up to, and including, fourth-order terms in any ϵ, γ combination. The $F_{0,i}$ terms are, of course, in agreement with those found by Larrain & Bonilla (1970). If we now examine the third-order axial flow, given by

$$\tilde{W} = \gamma^2\epsilon\tilde{W}_{21} + \gamma\epsilon^2\tilde{W}_{12} + \epsilon^3\tilde{W}_{03},$$

we see that it contains only terms proportional to $\sin n\theta$, and contributes nothing to the total flow rate, and that the first torsion-dependent contribution to the total flow rate arises from the constant part of $\tilde{W}_{2,2}$ and is proportional to $(\epsilon^2\gamma^2)$. In general, all torsional contributions to the total flow rate are proportional to $(\gamma^{2n}\epsilon^{2m})$, where

Terms	Angular dependence $\tilde{U}, \tilde{W}, \Pi$	$\tilde{V}$
F_{00}	1 ($\tilde{U}$ excepted)	none
F_{01}	none	none
F_{10}	$\sin\theta$	$\cos\theta$
F_{20}	none	none
F_{11}	$\cos\theta$	$\sin\theta$
F_{02}	$1, \cos 2\theta$	$\sin 2\theta$
F_{30}	none	none
F_{21}	$\sin\theta$	$\cos\theta$
F_{12}	$\sin 2\theta$	$1, \cos 2\theta$
F_{03}	$\sin\theta, \sin 3\theta$	$\cos\theta, \cos 3\theta$
F_{40}	none	none
F_{31}	$\cos\theta$	$\sin\theta$
F_{22}	$1, \cos 2\theta$	$\sin 2\theta$
F_{13}	$\cos\theta, \cos 3\theta$	$\sin\theta, \sin 3\theta$
F_{04}	$1, \cos 2\theta, \cos 4\theta$	$\sin 2\theta, \sin 4\theta$

TABLE 1. Angular dependences of terms in the perturbation expansion of the velocity field and the pressure

$n \geqslant 1$; this last condition is a consequence of the vanishing of all terms $F_{i,0}$. Thus calculation of the change in flow rate due to torsion requires the calculation of the constant part of $\tilde{W}_{2,2}$; details of this calculation are given in Appendix B. We finally find the following fractional change in flow rate from torsion effects as compared to the flow in a straight pipe:

$$\frac{\Delta Q_\tau}{Q_s} = \frac{\epsilon^2\gamma^2}{288}\left\{\left(\frac{\mathscr{R}^2}{288}\right)^3 \frac{(12\,483\,167)}{(140)^2(330)} - \left(\frac{\mathscr{R}^2}{288}\right)^2 \frac{(388\,817)}{(20)^2(105)} - \left(\frac{\mathscr{R}^2}{28}\right)\frac{8397}{140} + \frac{31}{8}\right\}. \tag{62}$$

We note that the change calculated here is only that due to torsion; the toroidal change has not been included, as it has been calculated by, for instance, Topakoglu (1967). According to this calculation, in cases where the first term dominates, the overall effect is of an increase in flow rate over that in a toroidal pipe of equal curvature.

It is important to remember that the results of this section apply only to pipes of strictly circular cross-section. For pipes of other cross-sections, the F_{10} terms do not vanish, and the effects of torsion appear in lower-order terms of the perturbation series (cf. the elliptical pipe of the previous section). In particular, for pipes of non-circular cross-section, one can expect to find contributions to the flow rate of order γ^2 alone. It is the rotational symmetry of the present case that causes the torsional effect to be pushed to a higher order in the perturbation series. This fortuitous circumstance also appears to have been the source of the confusion between the results obtained by Wang (1981) and Germano (1982). The streamtube cross-sections reported by Wang are those observed by an individual moving along the pipe and rotating with it in such a way that he is invariantly oriented with respect to the normal and binormal to the pipe axis. Germano's observer, on the other hand, also moves along the pipe axis, but rotates with respect to the normal and binormal. While this leaves the first-order terms (for the circular pipe) as the original Dean cells, calculation of the $(\epsilon\gamma)$ terms yields a transverse flow pattern which appears to

have sources and sinks. This is obscured by the velocity plots reported by Murata *et al.* (1981) and Kao (1987).

5. Conclusions and discussion

We have seen that the velocity field in a fixed frame can be written as the sum of three terms: a velocity along the pipe axis, a velocity seen by an observer travelling along the pipe axis and rotating with the Frenet triad, and a velocity representing the rotation of the Frenet triad, which is represented by $\boldsymbol{\omega} \times \boldsymbol{r}$, in agreement with elementary kinematics. The governing equations can be written in such a way that either the body-centred or the space-centred velocity components are the dependent variables; from these, one set of components can be found and the other easily generated by addition of the $\boldsymbol{\omega} \times \boldsymbol{r}$ term. The formulation given here is applicable not only to flow in helical pipes, but also to flow in pipes whose axes are straight but whose cross-sections precess about the pipe axis; these two problems are actually closely related.

The key to the question of whether torsion has a first- or second-order effect on the secondary flow in a helical pipe of circular cross-section is really only a question of the frame of reference of the observer; for a space-centred observer, the effect is of second order, while for a body-centred observer, the effect is of first order. While this result would seem to argue in favour of using a space-centred system for describing the secondary flow, consideration of pipes of cross-section other than circular and of higher-order terms for the case of a circular cross-section argue against it, as the streamtubes are not invariant in such a description. On the other hand, in the body-centred system, the streamtubes are invariant, and the secondary flow can be depicted in two dimensions. It is worth remembering that a streamtube is actually a two-dimensional surface embedded in a three-dimensional space, and a streamline is a directed line which itself is embedded in the two-dimensional surface described by the streamtube. Dean's recirculating cells of secondary flow are themselves only the projections on the pipe cross-section of the streamtube cross-sections, with arrows denoting the direction of circulation. Once this is realized, then it is clear that discussion of the effect of torsion on these cells must be made in a framework in which the streamtube projections can be found; this is clearly the body-centred formulation, as is easily seen from the continuity equation. From this we conclude that the coalescence of the two Dean cells owing to torsion is a first-order effect, in agreement with Wang's conclusions. The conclusion that the effect of torsion is of higher order, reached by Germano and Kao, is an accident of the symmetry of the cross-section chosen and does not hold up under analysis of higher-order terms, for which the concept of the projection of the streamtube cross-section onto the pipe cross-section is not relevant. This is particularly clear in cases where the pipe cross-section is not circular.

The author would like to thank the University of Exeter (UK) for its hospitality during a sabbatical leave during which much of this work was done. In particular, discussions of this work with Dr M. A. Patrick and the use of his contour plotting program are gratefully acknowledged.

Appendix A. Second-order calculation of the axial velocity in a straight elliptical pipe

The axial flow in second order is composed of two contributions: an inertial part, which we shall denote by $\tilde{W}_{2,\mathrm{I}}$, and a non-inertial part, which we shall denote by $\tilde{W}_{2,\mathrm{N}}$.

We consider the inertial part first. From (32d), we find that

$$\nabla^2\tilde{W}_{2,\mathrm{I}} = 2\mathscr{R}\left(-\frac{X}{A^2}\frac{\partial\Phi_2}{\partial Y}+\frac{Y}{B^2}\frac{\partial\Phi_2}{\partial X}\right), \tag{A 1}$$

where Φ_2 is given by (48) and (49). The solution to this equation must be of the form

$$\begin{aligned}\tilde{W}_{2,\mathrm{I}} = \left(1-\frac{X^2}{A^2}-\frac{Y^2}{B^2}\right)\Bigg(&A_1+A_2\frac{X^2}{A^2}+A_3\frac{Y^2}{B^2}+A_4\frac{X^4}{A^4}+A_5\frac{X^2Y^2}{A^2B^2}+A_6\frac{Y^4}{B^4}\\&+A_7\frac{X^6}{A^6}+A_8\frac{X^4Y^2}{A^4B^2}+A_9\frac{X^2Y^4}{A^2B^4}+A_{10}\frac{Y^6}{B^6}\\&+A_{11}\frac{X^8}{A^8}+A_{12}\frac{X^6Y^2}{A^6B^2}+A_{13}\frac{X^4Y^4}{A^4B^4}+A_{14}\frac{X^2Y^6}{A^2B^6}+A_{15}\frac{Y^8}{B^8}\Bigg).\end{aligned} \tag{A 2}$$

Upon substituting this form of $W_{2,\mathrm{I}}$ into (A 1) and matching coefficients, we can obtain equations for the 15 coefficients A_i in the form

$$\begin{aligned}&A_1\left(\frac{1}{A^2}+\frac{1}{B^2}\right) = Q_1, \quad A_2\left(\frac{6}{A^2}+\frac{1}{B^2}\right)+\frac{A_3}{B^2} = Q_2, \quad \frac{A_2}{A^2}+A_3\left(\frac{1}{A^2}+\frac{6}{B^2}\right) = Q_3,\\&A_4\left(\frac{15}{A^2}+\frac{1}{B^2}\right)+\frac{A_5}{B^2} = Q_4, \quad A_4\left(\frac{6}{A^2}\right)+A_5\left(\frac{6}{A^2}+\frac{6}{B^2}\right)+A_6\left(\frac{6}{B^2}\right) = Q_5,\\&\frac{A_5}{A^2}+A_6\left(\frac{1}{A^2}+\frac{15}{B^2}\right) = Q_6,\\&A_7\left(\frac{28}{A^2}+\frac{1}{B^2}\right)+\frac{A_8}{B^2} = Q_7, \quad A_7\left(\frac{15}{A^2}\right)+A_8\left(\frac{15}{A^2}+\frac{6}{B^2}\right)+A_9\left(\frac{6}{B^2}\right) = Q_8,\\&A_8\left(\frac{6}{A^2}\right)+A_9\left(\frac{6}{A^2}+\frac{15}{B^2}\right)+A_{10}\left(\frac{15}{B^2}\right) = Q_9, \quad \frac{A_9}{A^2}+A_{10}\left(\frac{1}{A^2}+\frac{28}{B^2}\right) = Q_{10},\\&A_{11}\left(\frac{45}{A^2}+\frac{1}{B^2}\right)+\frac{A_{12}}{B^2} = Q_{11}, \quad A_{11}\left(\frac{28}{A^2}\right)+A_{12}\left(\frac{28}{A^2}+\frac{6}{B^2}\right)+A_{13}\left(\frac{6}{B^2}\right) = Q_{12},\\&A_{12}\left(\frac{15}{A^2}\right)+A_{13}\left(\frac{15}{A^2}+\frac{15}{B^2}\right)+A_{14}\left(\frac{15}{B^2}\right) = Q_{13}, \quad A_{12}\left(\frac{6}{A^2}\right)+A_{13}\left(\frac{6}{A^2}+\frac{28}{B^2}\right)+A_{15}\left(\frac{28}{B^2}\right) = Q_{14},\\&\frac{A_{14}}{A^2}+A_{15}\left(\frac{1}{A^2}+\frac{45}{B^2}\right) = Q_{15},\end{aligned} \tag{A 3}$$

where the Q_i are given by

$$\begin{aligned}&Q_1 = \frac{A_2}{A^2}+\frac{A_3}{B^2}, \quad Q_2 = D_0+\frac{6}{A^2}A_4+\frac{A_5}{B^2}, \quad Q_3 = -D_0+\frac{A_5}{A^2}+\frac{6}{B^2}A_6,\\&Q_4 = -2D_0+D_y+\frac{15}{A^2}A_7+\frac{A_8}{B^2}, \quad Q_5 = -D_x+D_y+\frac{6}{A^2}A_8+\frac{6}{B^2}A_9,\end{aligned}$$

$$Q_6 = 2D_0 - D_y + \frac{A_9}{A^2} + \frac{15}{B^2}A_{10},$$

$$Q_7 = D_0 - 2D_x + \frac{28}{A^2}A_{11} + \frac{A_{12}}{B^2}, \quad Q_8 = D_0 - 2D_y + \frac{15}{A^2}A_{12} + \frac{6}{B^2}A_{13}, \tag{A 4}$$

$$Q_9 = -D_0 + 2D_x + \frac{6}{A^2}A_{13} + \frac{15}{B^2}A_{14}, \quad Q_{10} = -D_0 + 2D_y + \frac{A_{14}}{A^2} + \frac{28}{B^2}A_{15},$$

$$Q_{11} = D_x, \quad Q_{12} = D_x + D_y, \quad Q_{13} = -D_x + D_y, \quad Q_{14} = -D_x - D_y, \quad Q_{15} = -D_y,$$

and the quantities D_0, D_x, D_y are defined by

$$D_0 = -\frac{\Lambda\mathscr{R}}{AB}C_0, \quad D_x = -\frac{\Lambda\mathscr{R}}{AB}C_x, \quad D_y = -\frac{\Lambda\mathscr{R}}{AB}C_y, \tag{A 5}$$

Λ, C_0, C_x, and C_y having been defined in connection with the stream function Φ_2 in (49). The analytic solution of these equations for the A_i in terms of D_0, D_x, and D_y is exceedingly tedious and error-prone, so a slightly different approach has been used. It is relatively easy to find the coefficients in each group of coefficients in terms of the quantities Q_i defined in (A 4). The last five coefficients are now in the analytic form required, and can be substituted into the expressions for Q_7–Q_{10}, thus yielding solutions for the corresponding A_i. These results provide the input for Q_4–Q_6, etc. This program has been implemented by computer to give the results shown in figure 5(*b*). By careful use of the symmetry of the problem with respect to the interchange of X and Y and of A and B, it can be shown that $\tilde{W}_{2,\mathrm{I}}$ contributes nothing to the total flow rate. This result was reported earlier by Todd (1977) on the basis of computer calculations. We suspect that this will be true for any cross-section with two mutually perpendicular planes of reflection, but have not been able to establish this more general result.

We now turn to the non-inertial terms. The non-inertial part of W_2 satisfies the equation

$$\nabla^2 W_{2,\mathrm{N}} = -\gamma^2\left(Y\frac{\partial}{\partial X} - X\frac{\partial}{\partial Y}\right)^2 W_0 + \gamma\left(Y\frac{\partial}{\partial X} - X\frac{\partial}{\partial Y}\right)P_1, \tag{A 6}$$

where P_1 has been given by (36). This reduces to the form

$$\nabla^2 W_{2,\mathrm{N}} = \frac{12\gamma^2}{\Delta_1}\left(\frac{1}{A^2} - \frac{1}{B^2}\right)\left(\frac{1}{A^2} + \frac{1}{B^2}\right)^2 (X^2 - Y^2), \tag{A 7}$$

whose solution is

$$W_{2,\mathrm{N}} = \frac{2\gamma^2\left(\frac{1}{A^2} - \frac{1}{B^2}\right)\left(\frac{1}{A^2} + \frac{1}{B^2}\right)}{\Delta_1\left(\frac{1}{A^4} + \frac{6}{A^2B^2} + \frac{1}{B^4}\right)}\left(1 - \frac{X^2}{A^2} - \frac{Y^2}{B^2}\right)$$

$$\times\left[2\left(\frac{1}{A^2} - \frac{1}{B^2}\right) - \left(\frac{1}{A^4} + \frac{4}{A^2B^2} + \frac{3}{B^4}\right)X^2 + \left(\frac{3}{A^4} + \frac{4}{A^2B^2} + \frac{1}{B^4}\right)Y^2\right]. \tag{A 8}$$

This solution is shown in figure 5(*a*), and generates the second-order change in the total flow rate, as discussed in §3.

Appendix B. Calculation of the flow rate in a helical coil of circular cross-section

As outlined in §4, the lowest-order correction to the flow rate in a helical pipe of circular cross-section depends only on the angle-independent part of $\tilde{W}_{22}$, and is of $O(\epsilon^2\gamma^2)$. We denote this contribution by $\bar{W}_{22}$. Expansion of (53d) leads to the following equation for $\bar{W}_{22}$:

$$\begin{aligned}\frac{1}{\eta}\frac{\partial}{\partial\eta}\left(\eta\frac{\partial\bar{W}_{22}}{\partial\eta}\right) = {}& \epsilon\gamma\mathscr{R}\eta\sin\theta\frac{\partial\Pi_{11}}{\partial\theta}\bigg|_{\text{ave}} - \frac{\epsilon\sin\theta}{\eta}\frac{\partial}{\partial\eta}\left(\tilde{W}_{21}-\gamma\eta\frac{\partial\tilde{U}_{11}}{\partial\theta}\right)\bigg|_{\text{ave}} \\ & + \mathscr{R}\left\{\tilde{U}_{22}\frac{\partial\tilde{W}_{00}}{\partial\eta}+\tilde{U}_{21}\frac{\partial\tilde{W}_{01}}{\partial\eta}+\tilde{U}_{11}\frac{\partial\tilde{W}_{11}}{\partial\eta}+\tilde{U}_{01}\frac{\tilde{W}_{21}}{\partial\eta}\right. \\ & + \frac{1}{\eta}\left[\tilde{V}_{21}\frac{\partial\tilde{W}_{01}}{\partial\theta}+\tilde{V}_{11}\frac{\partial\tilde{W}_{11}}{\partial\theta}+\tilde{V}_{01}\frac{\partial\tilde{W}_{21}}{\partial\theta}\right]-\gamma\tilde{W}_{11}\frac{\partial\tilde{W}_{01}}{\partial\theta}-\gamma\tilde{W}_{01}\frac{\partial\tilde{W}_{11}}{\partial\theta} \\ & \left.+\epsilon\tilde{W}_{00}\left[\sin\theta\tilde{U}_{21}+\cos\theta\tilde{V}_{21}+\gamma\eta\sin\theta\frac{\partial\tilde{W}_{11}}{\partial\theta}\right]\right\}\bigg|_{\text{ave}}, \end{aligned} \tag{B 1}$$

which identifies the third-order terms that must be calculated. If we now make use of the fact that

$$\cos^2\theta = \tfrac{1}{2}(1+\cos 2\theta), \quad \sin^2\theta = \tfrac{1}{2}(1-\cos 2\theta),$$

and of the angular dependences given in table 1, then, after liberal use of the continuity equation, we can reduce (B 1) to the following form:

$$\begin{aligned}\frac{1}{\eta}\frac{\partial}{\partial\eta}\left(\eta\frac{\partial\bar{W}_{22}}{\partial\eta}\right) = {}& -\tfrac{1}{2}\mathscr{R}\eta\bar{\Pi}_{11}+\mathscr{R}\eta^3\frac{\partial}{\partial\eta}\left(\frac{\bar{U}_{22}}{\eta}\right) \\ & + \frac{1}{\eta}\frac{\partial}{\partial\eta}\{\eta[-\tfrac{1}{2}\bar{W}_{21}-\tfrac{1}{2}\eta\bar{U}_{11}+\tfrac{1}{2}\mathscr{R}(\bar{U}_{21}\bar{W}_{01}+\bar{U}_{11}\bar{W}_{11}+\bar{U}_{01}\bar{W}_{21}-2\bar{U}_{22})]\}, \end{aligned} \tag{B 2}$$

where the constant part of $\bar{U}_{22}$ required can be obtained from the continuity equation

$$\frac{\partial}{\partial\eta}(\eta\bar{U}_{22})-\frac{\partial}{\partial\eta}(\epsilon\eta^2\sin\theta\tilde{U}_{21})\,|_{\text{ave}} = 0, \tag{B 3}$$

and the bars over the quantities on the right-hand sides indicate that only the radial dependence is to be considered.

It is also convenient to factor out as many powers of (η^2-1) as possible from each of the contributing terms. These have the following form:

$$\bar{U}_{01} = \frac{\mathscr{R}(\eta^2-1)^2}{(288)}(-\eta^2+4),$$

$$\bar{U}_{11} = \tfrac{1}{6}(\eta^2-1)^2+\frac{\mathscr{R}^2}{(288)(240)}(\eta^2-1)^2(-\eta^6+7\eta^4-15\eta^2+13),$$

$$\begin{aligned}\bar{U}_{21} = {}& \frac{\mathscr{R}}{(288)(480)}(\eta^2-1)^2(-102\eta^4+276\eta^2+1134) \\ & + \frac{\mathscr{R}^3}{(288)^2(140)^2 6}(\eta^2-1)^2(375\eta^{10}-3702\eta^8+13389\eta^6 \\ & -20979\eta^4+4941\eta^2+33792), \end{aligned}$$

$$\bar{U}_{22} = \frac{\mathscr{R}}{(288)(160)}(\eta^2-1)^2(17\eta^5-46\eta^3-189\eta)$$
$$+\frac{\mathscr{R}^3}{(288)^2(280)^2}(\eta^2-1)^2(-125\eta^{11}+1234\eta^9-4463\eta^7$$
$$+6990\eta^5-1647\eta^3-11264\eta),$$
$$\bar{W}_{01} = \tfrac{1}{4}(\eta^2-1)(3\eta)+\frac{\mathscr{R}^2}{(288)(40)}(\eta^2-1)(\eta^7-9\eta^5+21\eta^3-19\eta), \tag{B 4}$$
$$\bar{W}_{11} = \frac{\mathscr{R}}{(288)2}(\eta^2-1)(3\eta^5-5\eta^3-29\eta)$$
$$+\frac{\mathscr{R}^3}{(288)^2(350)}(\eta^2-1)(20\eta^{11}-274\eta^9+1301\eta^7-3249\eta^5+4381\eta^3-2969\eta),$$
$$\bar{W}_{21} = \tfrac{1}{96}(\eta^2-1)(5\eta^3-6\eta)$$
$$+\frac{\mathscr{R}^2}{(288)(960)}(\eta^2-1)(-8\eta^9+25\eta^7+190\eta^5-658\eta^3+774\eta)$$
$$+\frac{\mathscr{R}^4}{(288)^2(280)^2(24)}(\eta^2-1)(-415\eta^{15}+7757\eta^{13}-56083\eta^{11}$$
$$+232037\eta^9-620567\eta^7+1065233\eta^5-1162699\eta^3+697301),$$
$$\bar{\Pi}_{11} = \frac{1}{6\mathscr{R}}(\eta^3-\eta)+\frac{\mathscr{R}}{(240)(72)}(3\eta^9-30\eta^7+90\eta^5-120\eta^3+101\eta).$$

After solving (B 2) for $\bar{W}_{22}$ and integrating the result over the pipe cross-section to find the change in flow rate, we obtain the result given in (62).

REFERENCES

BATCHELOR, G. K. 1967 *An Introduction to Fluid Dynamics*, Appendix 2. Cambridge University Press.

BERGER, S. A., TALBOT, L. & YAO, L. S. 1983 Flow in curved pipes. *Ann. Rev. Fluid Mech.* **15**, 461–512.

DEAN, W. R. 1927 Note on the motion of fluid in a curved pipe. *Phil. Mag.* **4** (7), 208–223.

DEAN, W. R. 1928 The stream-line motion of fluid in a curved pipe. *Phil. Mag.* **5** (7), 673–695.

GERMANO, M. 1982 On the effect of torsion on a helical pipe flow. *J. Fluid Mech.* **125**, 1–8.

ITO, H. 1987 Flow in curved pipes. *JSME Intl J.* **30**, 543–552.

KAO, H. C. 1987 Torsion effect on fully developed flow in a helical pipe. *J. Fluid Mech.* **184**, 335–356.

LARRAIN, J. & BONILLA, C. F. 1970 Theoretical analysis of pressure drop in the laminar flow of fluid in a coiled pipe. *Trans. Soc. Rheol.* **14**, 135–147.

MANLAPAZ, R. L. & CHURCHILL, S. W. 1980 Fully developed laminar flow in a helically coiled tube of finite pitch. *Chem. Engng Commun.* **7**, 57–78.

MURATA, S., MIYAKE, Y., INABA, T. & OGATA, H. 1981 Laminar flow in a helically coiled pipe. *Bull. JSME* **24**, 355–362.

TODD, L. 1977 Some comments on steady, laminar flow through twisted pipes. *J. Engng Maths* **11**, 29–48.

TOPAKOGLU, H. C. 1967 Steady laminar flows of an incompressible viscous fluid in curved pipes. *J. Math. Mech.* **16**, 1321–1338.

TRUESDELL, L. C. & ADLER, R. J. 1970 Numerical treatment of fully developed laminar flow in helically coiled tubes. *AIChE J.* **16**, 1010–1015.

WANG, C. Y. 1981 On the low-Reynolds-number flow in a helical pipe. *J. Fluid Mech.* **108**, 185–194.